Supporting information for

Modulation of triplet-mediated emission from selenoxanthen-9-one-based D-A-D type emitters through tuning twist angle to realize electroluminescence efficiency over 25%

Xianchao Han,[ab] Xin Wang,[ab] Yuliang Wu,[ab] Jingcheng Zhao,[ab] Yang Liu,[ab] Haiyang Shu,[ab] Xiaofu Wu,[a] Hui Tong*[ab] and Lixiang Wang*[ab]

[a] State Key Laboratory of Polymer Physics and Chemistry, Changchun Institute of Applied Chemistry, Chinese Academy of Sciences, Changchun 130022, China
[b] School of Applied Chemistry and Engineering, University of Science and Technology of China, Hefei 230026, China

Corresponding Author
* E-mail: chemtonghui@ciac.ac.cn; lixiang@ciac.ac.cn

Table of Contents

Experimental section

Measurements and characterization. ^{1}H NMR and ^{13}C NMR spectroscopy were recorded at 500 MHz (Bruker AV) with TMS as the internal standard. All chemical shifts are given in ppm and all coupling constants (*J* values) are reported in Hertz (Hz). High-resolution mass spectra were obtained by using LTQ Orbitrap Velos Pro. Thermal gravimetric analyses were performed on TA-TGA55 under N_2 atmosphere at a heating rate of 15 ^{o}C/min, in which the decomposition temperature (T_d) is defined as the temperature at which the material showed a 5% weight loss. Differential scanning calorimetry (DSC) were performed on PerkinElmer-DSC 7 under N_2 atmosphere at a heating rate of 15°C/min. The UV-vis absorption spectra were recorded on a Perkin-Elmer Lambda 35 UV-Vis spectrometer. The HOMO and LUMO energy levels were investigated through the cyclic voltametric (CV) properties. Cyclic voltametric (CV) measurements were carried out by using a CHI610E electrochemical analyzer with 0.1 mol/L $[(n\text{-}Bu)_4N]ClO_4$ as supporting electrolyte in solution at room temperature. The ferrocenium/ferrocene was used as the internal reference. $Ag/AgNO_3$ electrode, glassy carbon electrode and platinum wire were used as the reference, working and counter electrode, respectively. Dichloromethane (DCM) was used for the measurement of oxidation potential while Tetrahydrofuran (THF) was adopted for reduction potential. Steady-state PL spectra, phosphorescence spectra and transient PL decay curves were measured on an Edinburgh FLSP-980 fluorescence spectrophotometer. Fluorescence lifetime is using a 375 nm picosecond pulsed LED (EPL375) as the excitation source and time correlated single photon counting (TCSPC) as data acquisition technique. Phosphorescence lifetime is using a 60 W xenon flashlamp (μF2) as the excitation source and multi-channel scaling (MCS) for time resolved photon counting as data acquisition technique. Time-resolved emission spectra (TRES) were measured on an Edinburgh FLSP-980 fluorescence spectrophotometer equipped with a 375 nm picosecond pulsed LED (EPL375). The PLQYs were measured on an integrating sphere (Hamamatsu Photonics C9920-2).

Single-Crystal Structure. The single crystals of CzSe and TMCzSe were cultivated by the solvent diffusion method in toluene and n-hexane. The single crystal X-ray diffraction experiments were carried out using a Bruker Smart APEX diffractometer with CCD area detector and graphite monochromator, Mo Kα radiation (λ =0.71073 Å). The intensity data were recorded with ω scan mode. Lorentz, polarization factors were made for the intensity data and absorption corrections were performed using SADABS program. The crystal structure was determined using the SHELXTL program and refined using full matrix least squares. All non-hydrogen atoms were assigned with anisotropic displacement parameters, whereas hydrogen atoms were placed at calculated positions theoretically and included in the final cycles of refinement in a riding model along with the attached carbons. Thus, obtained crystallographic parameters of CzSe and TMCzSe were summarized in Table S3 and CCDC reference number is 2155252 and 2155251.

Theoretical calculations. All the density functional theory (DFT) and time-dependent DFT (TD-DFT) calculations were performed with the Gaussian 09 program suite.[1] The ground-state (S_0) geometries of the two compounds were optimized by PBE0/TZVP level. Based on the optimized S_0 structures, TD-DFT calculations at PBE0/TZVP level were carried out to investigate the excited state properties of the two compounds. The orbital coupling constant (SOC) were carried out at the PBE0/TZVP level using on ORCA 4.1.0.[2] The SOC is calculated using optimized S_0/T_1 geometry. The hole and electron distribution analysis is performed by Multiwfn program. [3]

Device fabrication and testing. The device configuration is ITO/TAPC (90 nm)/TCTA (5 nm)/mCBP:x wt.% Emitter (30 nm)/TSPO1(5 nm)/TmPyPB (45 nm)/LiF (1 nm)/Al (150 nm). Here, ITO and Al were acted as anode and cathode, respectively. TAPC were used as the hole injection layer and hole transporting layer. TCTA was employed as the exciton-blocking layer. LiF and TmPyPB were utilized as the electron injection layer and electron transporting layer. TSPO1 was employed as

the exciton-blocking layer. The devices were prepared in vacuum at a pressure of 4×10^{-4} Pa. All organic layers were thermally evaporated at a rate of 1.5 Å/s. After the organic film deposition, 1 nm of LiF and 150 nm of aluminum were thermally evaporated onto the organic surface. Current density-voltage-luminance characteristics and electroluminescence (EL) spectra were measured using a Keithley source measurement unit (Keithley 2400 and Keithley 2000) and a CS2000 spectra colorimeter. All the devices were measured under ambient atmosphere. EQE were calculated on the basis of the EL spectrum, luminance and current density assuming a Lambertian emission distribution.

Synthesis

All reagents were purchased from commercial channels, and used directly unless specifically mentioned. Toluene and N, N-dimethylformamide (DMF) were dried respectively beforehand according to the standard procedures. 1,2-bis(3-bromophenyl) diselane was synthesized according to the literature procedures. [4]

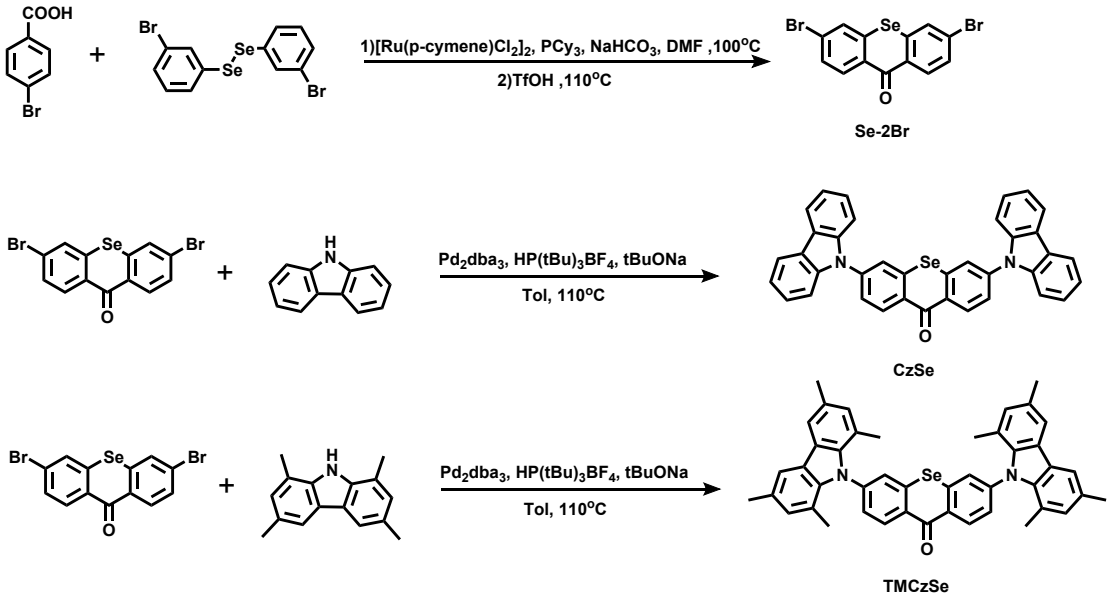

Scheme S1. Synthesis of CzSe and TMCzSe

Synthesis of 3,6-dibromo-9H-selenoxanthen-9-one (Se-2Br)

4-Bromobenzoic acid (3 g, 15 mmol), 1,2-bis(3-bromophenyl)diselane (7.07 g, 15 mmol), [Ru(*p*-cymene)Cl_2]$_2$ (390 mg, 0.60 mmol), PCy_3 (336 mg, 1.2 mmol), and $NaHCO_3$ (1.26 g, 15 mmol) were dissolved in dry DMF (80 mL) under air, and the resulting mixture was heated at 100 °C for 48 h. The colour changes from orange to deep-red and then becomes black. Acetic acid was added to adjust the solution to acidity, and then diluted with water. The mixture was extracted with ethyl acetate, and then washed with saturated brine. After the organic layer was dried over anhydrous $NaSO_4$, the solvent was removed under vacuum. The residue was purified by silica gel column chromatography (n-hexane: ethyl acetate: acetic acid = 90: 10: 1) to get the crude product, which was further treated with triflic acid at 100 °C for 5 h. After cooling to room temperature, the reaction was quenched with water, and then extracted with

dichloromethane (DCM). The organic layer was dried over anhydrous Na_2SO_4 and concentrated under reduced pressure. The crude product was purified by column chromatography on silica gel using dichloromethane/cyclohexane as the eluent to afford a white solid (1.69 g, 27%).^{1}H NMR (500 MHz, $CDCl_3$, δ ppm): 8.47 (d, *J* = 8.7 Hz, 2H), 7.83 – 7.76 (m, 2H), 7.60 (dd, *J* = 8.6, 1.9 Hz, 2H). ^{13}C NMR (126 MHz, $CDCl_3$, δ ppm) :180.67, 135.92, 132.91, 130.57, 130.48, 129.40, 128.08.

Synthesis of 3,6-di(9H-carbazol-9-yl)-9H-selenoxanthen-9-one (CzSe)

A mixture of 9H-carbazole (735 mg, 4.4 mmol), 3,6-dibromo-9H-selenoxanthen-9-one (836 mg, 2 mmol), Pd_2dba_3 (366 mg, 0.4 mmol), t-Bu_3PHBF_4 (348 mg, 1.2 mmol), t-BuONa (768 mg, 8 mmol) and anhydrous toluene (50 mL) was added into a two-neck round bottom flask. The mixture was heated to reflux overnight under an argon atmosphere. After cooling to room temperature, the mixture was extracted with deionized water and dichloromethane, and dried over anhydrous Na_2SO_4. After removal of the solvent under reduced pressure, the crude product was purified by column chromatography on silica gel using dichloromethane/petroleum ether as the eluent to afford a yellow solid (672 mg, 57%).^{1}H NMR (500 MHz, $CDCl_3$, δ ppm):8.94 (d, *J*=8.6 Hz, 2H), 8.16 (d, *J*=7.7 Hz, 4H), 7.96 – 7.90 (m, 2H), 7.79 (dd, *J*=8.6, 2.0 Hz, 2H), 7.58 (d, *J*=8.2 Hz, 4H), 7.51 – 7.43 (m, 4H), 7.35 (dd, *J*=11.0, 3.9 Hz, 4H). ^{13}C NMR (126 MHz, $CDCl_3$, δppm): 180.20, 141.62, 139.98, 133.35, 126.40, 125.13, 124.08, 121.01, 120.59, 109.82. HRMS (MALDI) m/z calcd: 590.1 $[M]^+$; found: 590.1 $[M]^+$.

Synthesis of 3,6-bis(1,3,6,8-tetramethyl-9H-carbazol-9-yl)-9H-selenoxanthen-9-one (TMCzSe)

A mixture of 1,3,6,8-tetramethyl-9H-carbazole (982 mg, 4.4 mmol), 3,6-dibromo-9H-selenoxanthen-9-one (836 mg, 2 mmol), Pd_2dba_3 (366 mg, 0.4 mmol), t-Bu_3PHBF_4 (348 mg, 1.2 mmol), t-BuONa (768 mg, 8 mmol) and anhydrous toluene (50 mL) was added into a two-neck round bottom flask. The mixture was heated to reflux overnight under an argon atmosphere. After cooling to room temperature, the mixture was

extracted with deionized water and dichloromethane, and dried over anhydrous Na_2SO_4. After removal of the solvent under reduced pressure, the crude product was purified by column chromatography on silica gel using dichloromethane/petroleum ether as the eluent to afford a yellow solid (912 mg, 65%).^{1}H NMR (500 MHz, $CDCl_3$, δ ppm): 8.79 (d, *J*=8.4 Hz, 2H), 7.75 (s, 4H), 7.69 (d, *J*=1.8 Hz, 2H), 7.67 (dd, *J*=8.4, 2.0 Hz, 2H), 6.93 (s, 4H), 2.48 (s, 12H), 1.93 (s, 12H).^{13}C NMR (126 MHz, $CDCl_3$, δ ppm) :180.76, 146.63, 139.62, 134.64, 131.57, 130.53, 130.46, 130.40, 130.07, 129.81, 124.74, 121.18, 117.99, 21.09, 19.78. HRMS (MALDI) m/z calcd: 702.2 $[M]^+$; found: 702.2$[M]^+$.

Thermal characterization

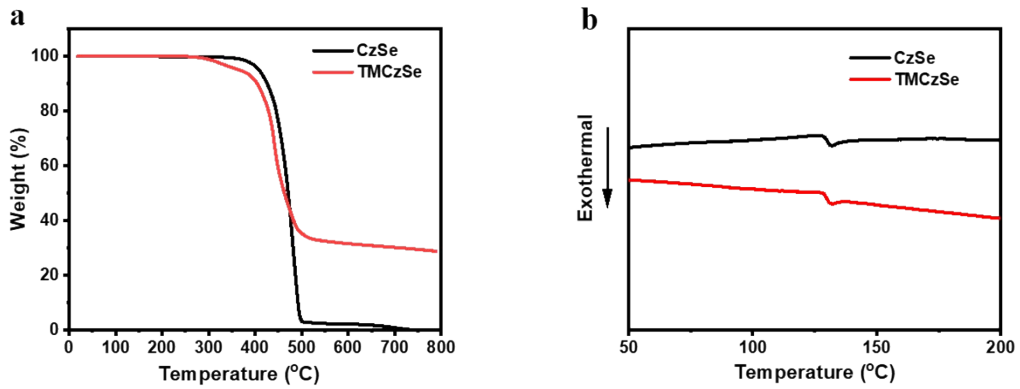

Figure S1. TGA (**a**) and DSC curves (**b**) of CzSe and TMCzSe.

Table S1. Thermal properties for TMCzSe and CzSe.

Compound	T_g [°C]	T_d [°C] [a]
CzSe	**131**	**409**
TMCzSe	**132**	**367**

[a] T_d were determined at 5% weight loss.

Electrochemical characterization

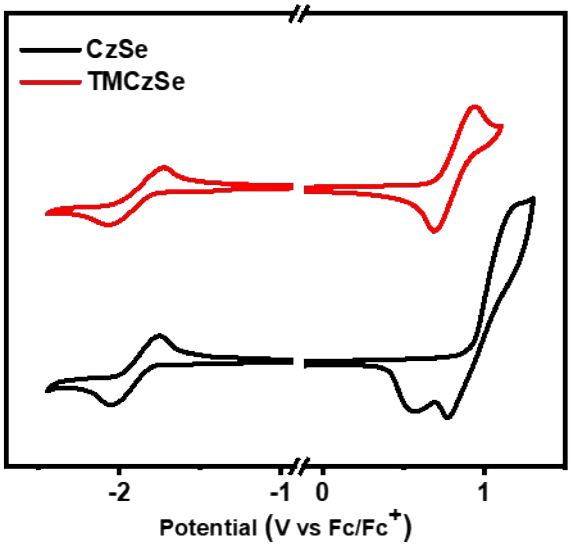

Figure S2. CV curves of CzSe and TMCzSe.

Photophysical characterization

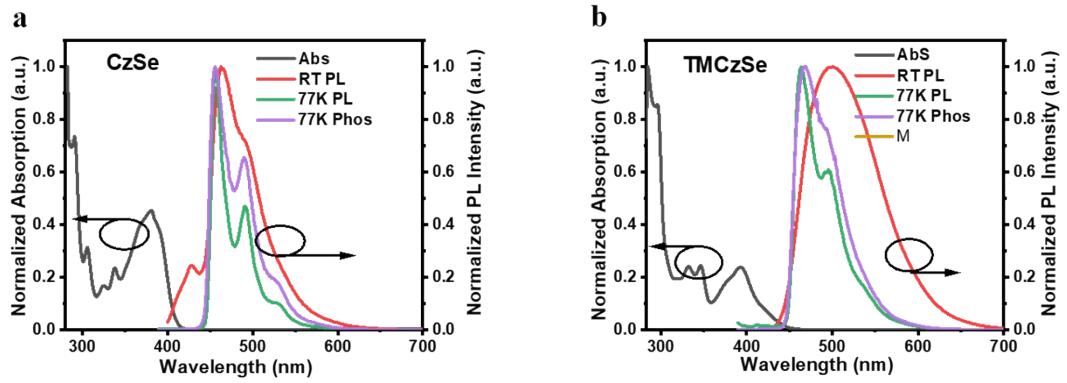

Figure S3. UV-vis absorption spectra, PL spectra at room temperature, PL spectra and phosphorescence spectra (with a 1 ms delay) at 77K of CzSe (**a**) and TMCzSe (**b**) measured in toluene (10^{-5} mol L^{-1}) under air.

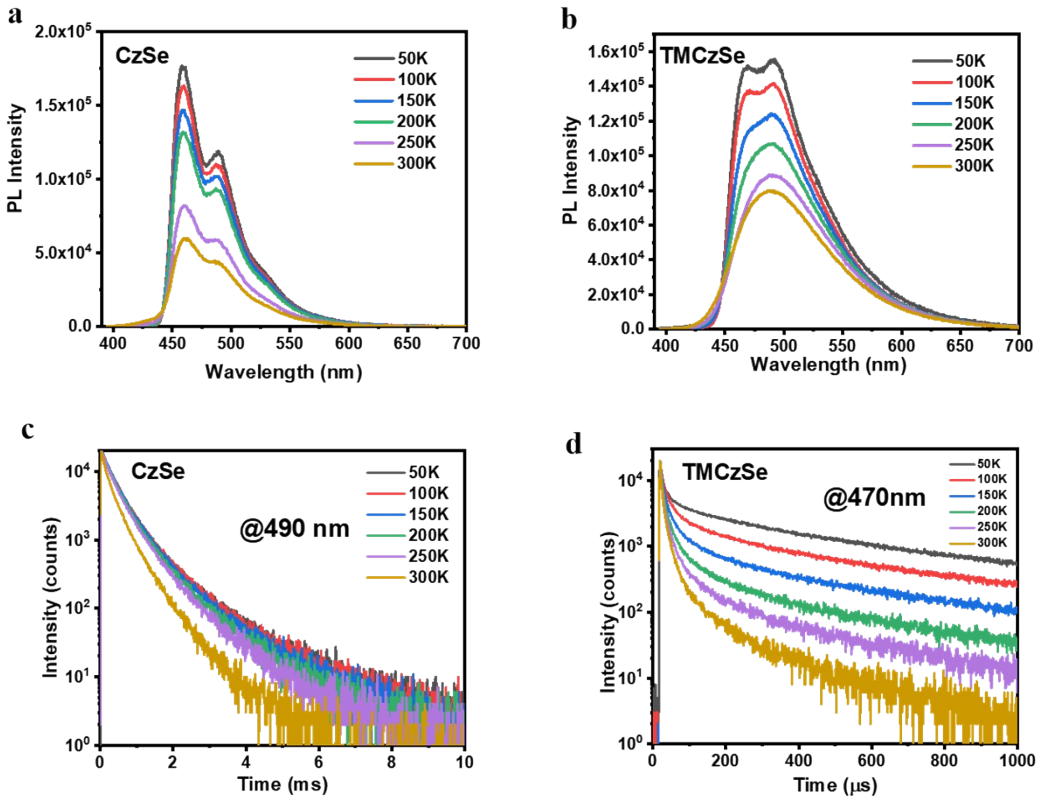

Figure S4. Steady-state PL spectra in the 1 wt.% doped PMMA films measured at different temperatures of CzSe(**a**) and TMCzSe (**b**); Temperature-dependent transient PL spectra in the 1 wt.% doped PMMA films measured at different temperatures of CzSe(**a**) and TMCzSe (**b**). All measures are in vacuum.

To better understand the exciton dynamic process, the radiative rate constants of phosphorescence (k_r^p) and the nonradiative constant of phosphorescence (k_{nr}^p) of the CzSe doped PMMA films were calculated using the following equations:

$k_r^p = \Phi_p / \tau_p$ $\quad$ $k_{nr}^p = (1- \Phi_p) / \tau_p$

k_r^p and k_{nr}^p of CzSe doped film are 8.7×10^2 and 1.91×10^3 s^{-1}, respectively.

Table S2. Lifetime data of TMCzSe in doped PMMA film with a concentration of 1 wt.%. They are obtained using the three-exponential decay functions $\tau=B_1\tau_1+ B_2\tau_2+ B_3\tau_3$.

T (K)	τ (μs)	τ_1 (μs)	B_1 (%)	τ_2 (μs)	B_2 (%)	τ_3 (μs)	B_3 (%)
300	26.71	3.00	31.46	15.15	53.41	116.85	15.13
250	48.99	3.72	29.51	18.40	46.51	164.05	23.98
200	71.15	4.06	24.72	20.62	41.37	181.65	33.92
150	120.40	4.75	19.50	24.37	33.43	236.51	47.07
100	179.23	5.45	14.80	28.69	23.70	279.07	61.50
50	267.21	6.77	9.31	33.65	12.64	336.10	78.05

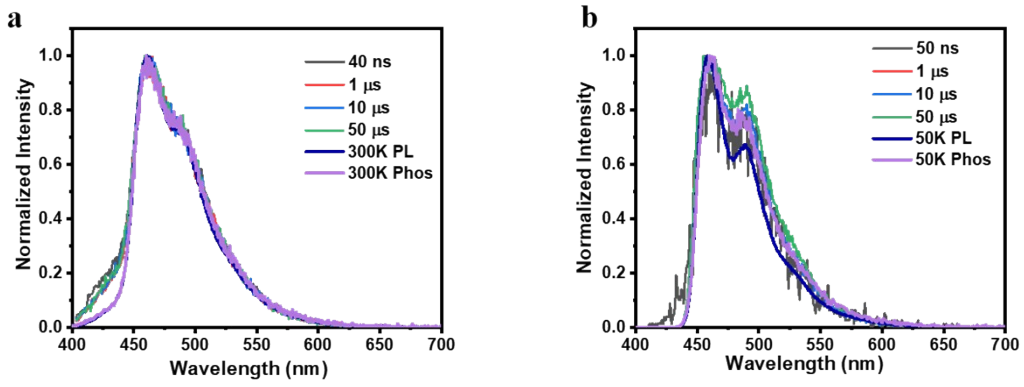

Figure S5. Time-resolved emission spectra (TRES) at different temperature compared with steady-state PL and room temperature phosphorescence spectra in the 1 wt.% doped PMMA film of CzSe. **a.** 300 K; **b.** 50 K.

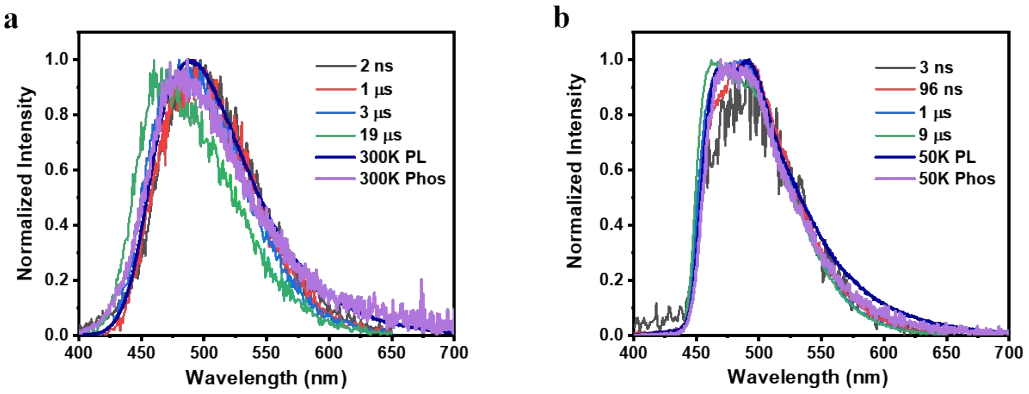

Figure S6. Time-resolved emission spectra (TRES) at different temperature compared with steady-state PL and room temperature phosphorescence spectra in the 1 wt.% doped PMMA film of TMCzSe. **a.** 300 K; **b.** 50 K.

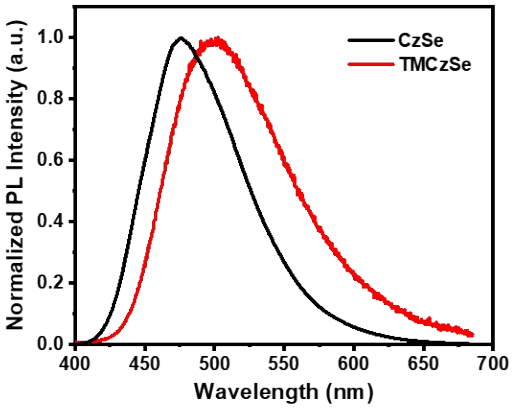

Figure S7. Steady-state PL spectra at room temperature for the doped film in mCBP of CzSe and TMCzSe in vacuum (CzSe: 5 wt.% doped in mCBP; TMCzSe: 10 wt.% doped in mCBP).

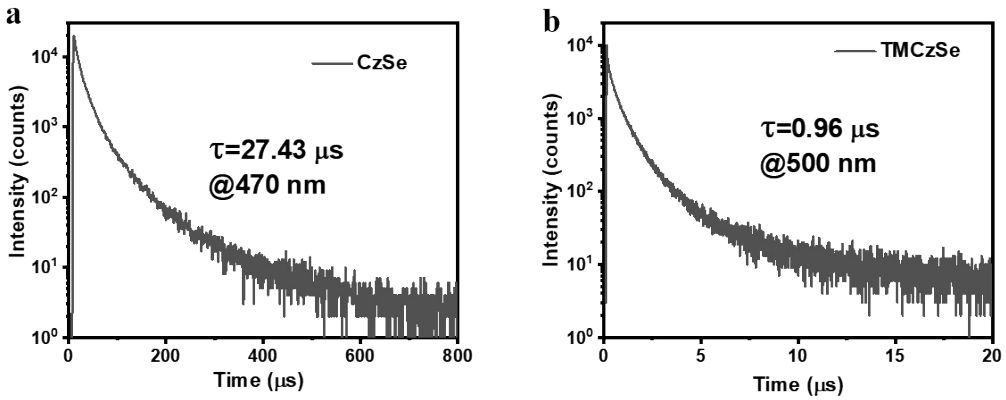

Figure S8. Transient PL spectra for the doped films in mCBP of CzSe(**a**) and TMCzSe (**b**) in vacuum at room temperature (CzSe: 5 wt.% doped in mCBP; TMCzSe: 10 wt.% doped in mCBP).

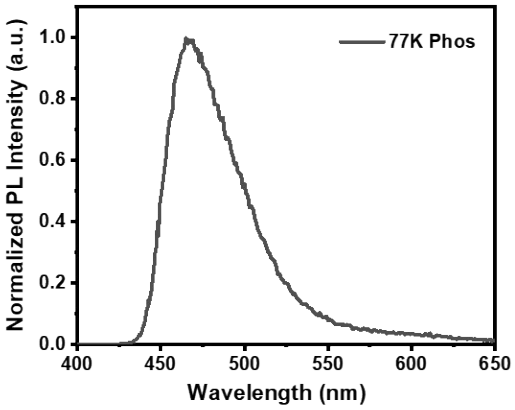

Figure S9. Phosphorescence spectra at 77 K (with a 0.5 ms delay) for the the 1 wt.% doped PMMA film of **Selenoxanthen-9-one** under air.

X-ray crystallographic analysis

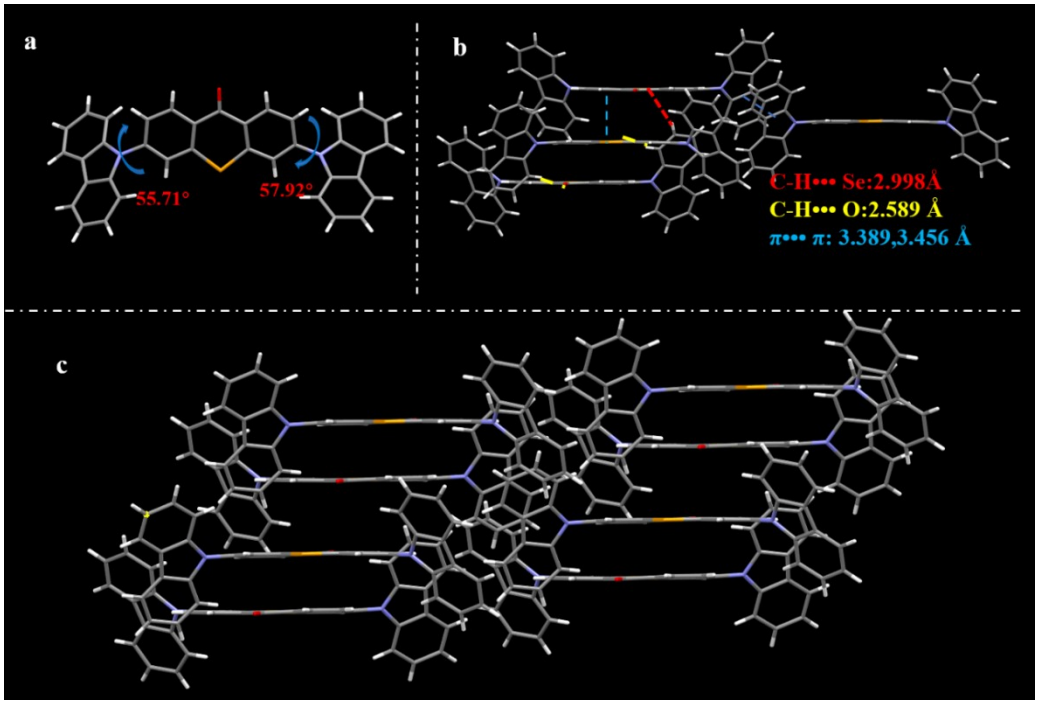

Figure S10. Single crystal structure of CzSe and associated intermolecular interactions.

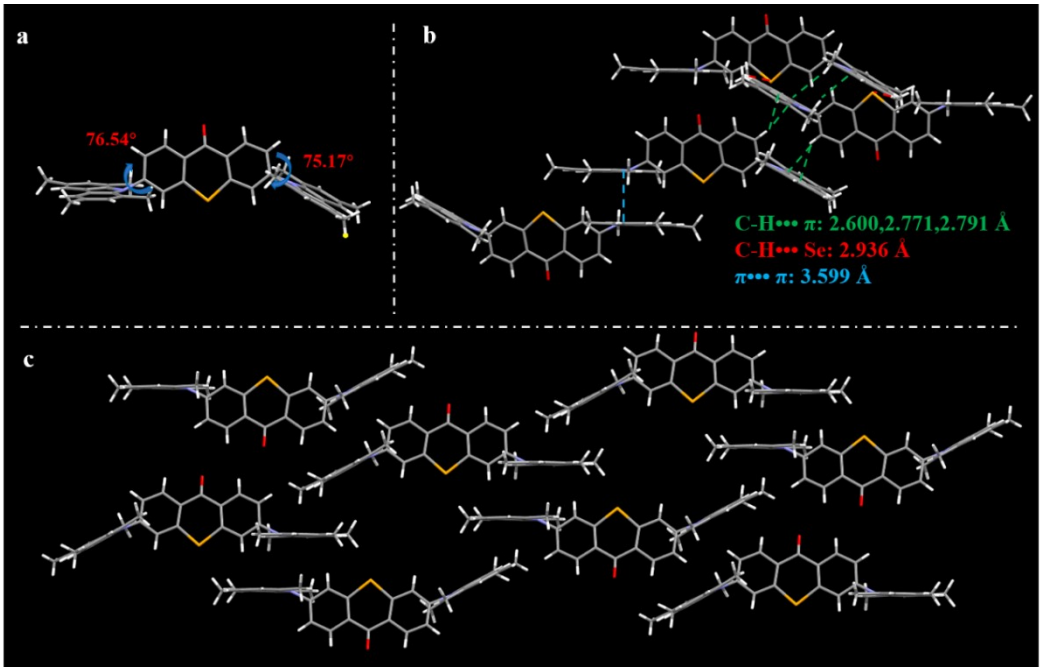

Figure S11. Single crystal structure of TMCzSe and associated intermolecular interactions.

Table S3. Single crystal data of CzSe and TMCzSe.

Compound	CzSe	TMCzSe
Empirical formula	$C_{37}H_{22}N_2OSe$	$C_{45}H_{38}N_2OSe$
Formula weight	589.53	701.73
Temperature	260.0 K	173.0 K
Crystal system	Triclinic	Triclinic
Space group	P-1	P-1
Unit cell dimensions	a=9.090(2) Å b=9.925(2) Å c=14.588(3) Å α=95.004(8) β=90.725(8) γ =92.922(8)	a= 10.0627(7) Å b= 11.3393(8) Å c= 16.4880(11) Å α =95.860(2) β=98.152(2) γ =93.116(2)
Volume	1309.2(5) $Å^3$	1848.1(2) $Å^3$
Z	2	2
Density	1.495	1.261
F (000)	600.0	728.0
2θ range for data collection	2.06 to 37.89°	2.050 to 30.694°
Index ranges	-15≤ h ≤ 15, -17 ≤ k ≤ 17, -25 ≤ l ≤ 25	-14 ≤ h ≤ 14, -16 ≤ k ≤ 16, -23 ≤ l ≤ 23
Reflections collected	104773	77008
Independent reflections	13921 [R_{int} = 0.0964]	11386 [R_{int} = 0.0662]
Data/restraints/parameters	13921/0/370	11386/0/442
Goodness-of-fit on F^2	1.118	1.044
Final R indexes [I>=2σ (I)]	R_1 = 0.0645, wR_2 = 0.1788	R_1 = 0.0526, wR_2 = 0.1578
Final R indexes [all data]	R_1 = 0.0964, wR_2 = 0.1883	R_1 = 0.0662, wR_2 = 0.1655
CCDC	2155252	2155251

Theoretical calculation

Table S4. SOC constant of CzSe calculated using optimized S_0 geometry.

	SOC (cm^{-1})
$\zeta(T_1,S_0)$	2.93
$\zeta(S_1,T_1)$	15.31
$\zeta(S_1,T_2)$	0.50
$\zeta(S_1,T_3)$	18.53
$\zeta(S_1,T_4)$	0.16
$\zeta(S_1,T_5)$	0.65
$\zeta(S_1,T_6)$	3.39

Table S5. SOC constant of TMCzSe calculated using optimized S_0 geometry.

	SOC (cm^{-1})
$\zeta(T_1,S_0)$	3.50
$\zeta(S_1,T_1)$	4.92
$\zeta(S_1,T_2)$	0.19
$\zeta(S_1,T_3)$	20.07

Table S6. Energy levels of CzSe calculated using optimized S_0 geometry.

Excited state	Energy level (eV)
S_1	2.6252
T_1	2.5568
T_2	2.5805
T_3	2.7367

Table S7. Energy levels of TMCzSe calculated using optimized S_0 geometry.

Excited state	Energy level (eV)
S_1	3.1587
T_1	2.6998
T_2	2.8405
T_3	3.0003
T_4	3.0913
T_5	3.0914
T6	3.1915

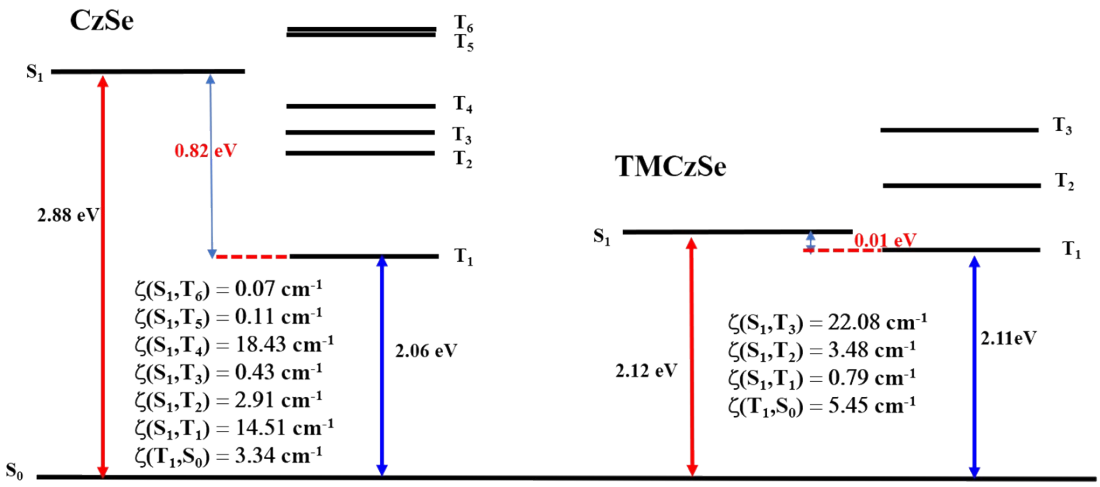

Figure S12. Calculated energy diagram and spin-orbital coupling (ζ) at the T_1-geomrtry

Table S8. SOC constant of CzSe calculated using optimized T_1 geometry.

	SOC (cm^{-1})
$\zeta(T_1,S_0)$	3.34
$\zeta(S_1,T_1)$	14.51
$\zeta(S_1,T_2)$	2.91
$\zeta(S_1,T_3)$	0.43
$\zeta(S_1,T_4)$	18.43
$\zeta(S_1,T_5)$	0.11
$\zeta(S_1,T_6)$	0.07

Table S9. SOC constant of TMCzSe calculated using optimized T_1 geometry.

	SOC (cm^{-1})
$\zeta(T_1,S_0)$	5.45
$\zeta(S_1,T_1)$	0.79
$\zeta(S_1,T_2)$	3.48
$\zeta(S_1,T_3)$	22.08

Table S10. Energy levels of CzSe calculated using optimized T_1 geometry.

Excited state	Energy level (eV)
S_1	2.8751
T_1	2.0585
T_2	2.5646
T_3	2.7400
T_4	2.8751
T_5	3.0421
T6	3.0422

Table S11. Energy levels of TMCzSe calculated using optimized T_1 geometry.

Excited state	Energy level (eV)
S_1	2.1192
T_1	2.1098
T_2	2.3196
T_3	2.4578

Device characterization

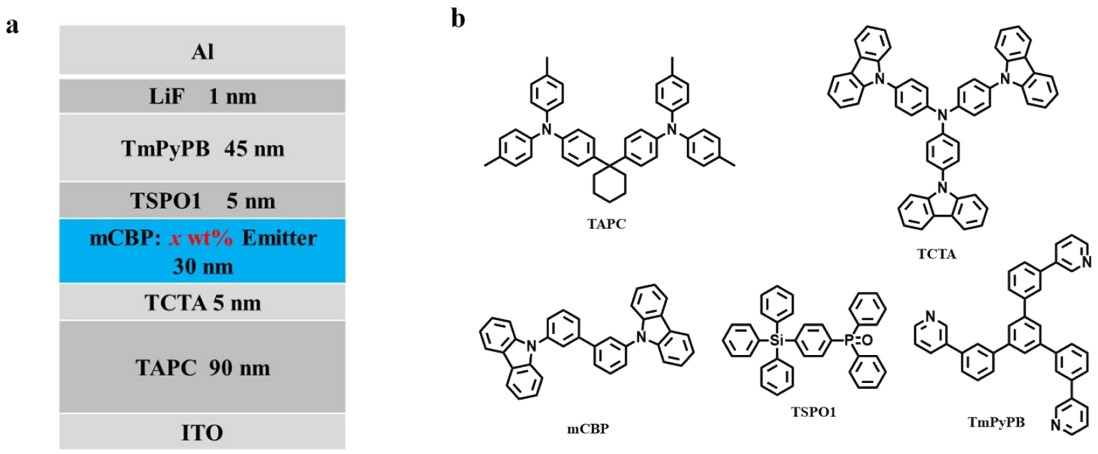

Figure S13. a. Device configuration of OLEDs; **b.** The molecular structures of used materials.

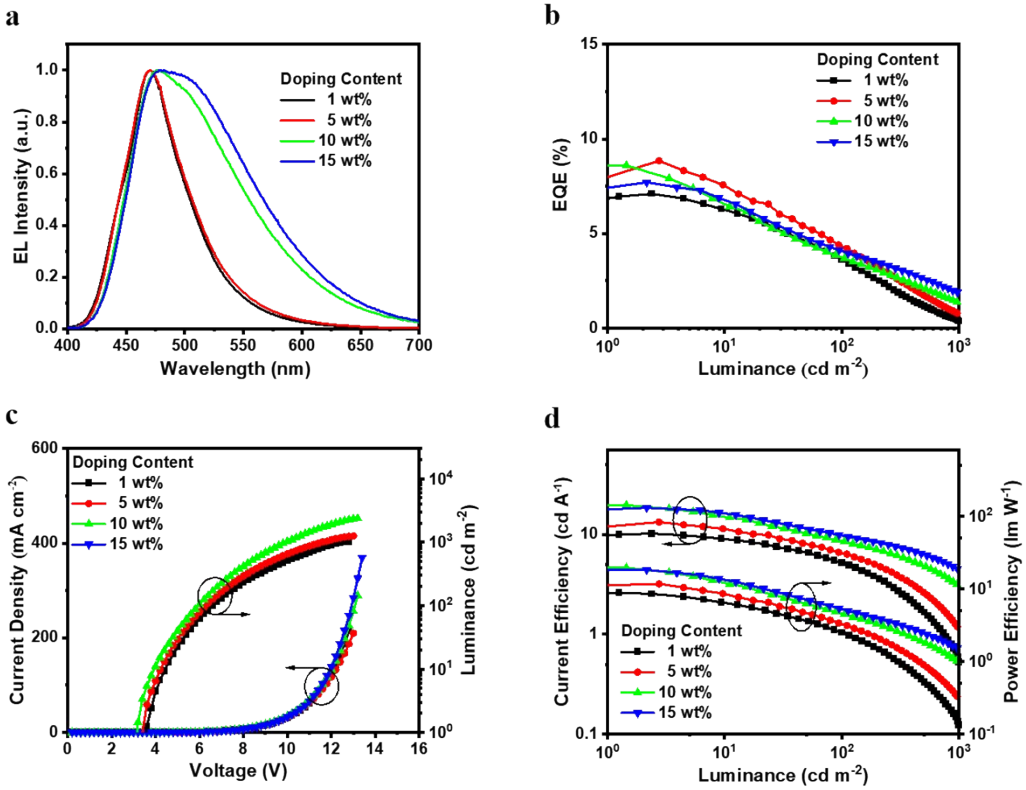

Figure S14. For CzSe of different doping contentrations in mCBP, **a.** Normalized EL spectrum; **b.** EQE as a function of luminance; **c.** Current density-voltage-luminance characteristics; **d.** Current efficiency and power efficiency as a function of luminance.

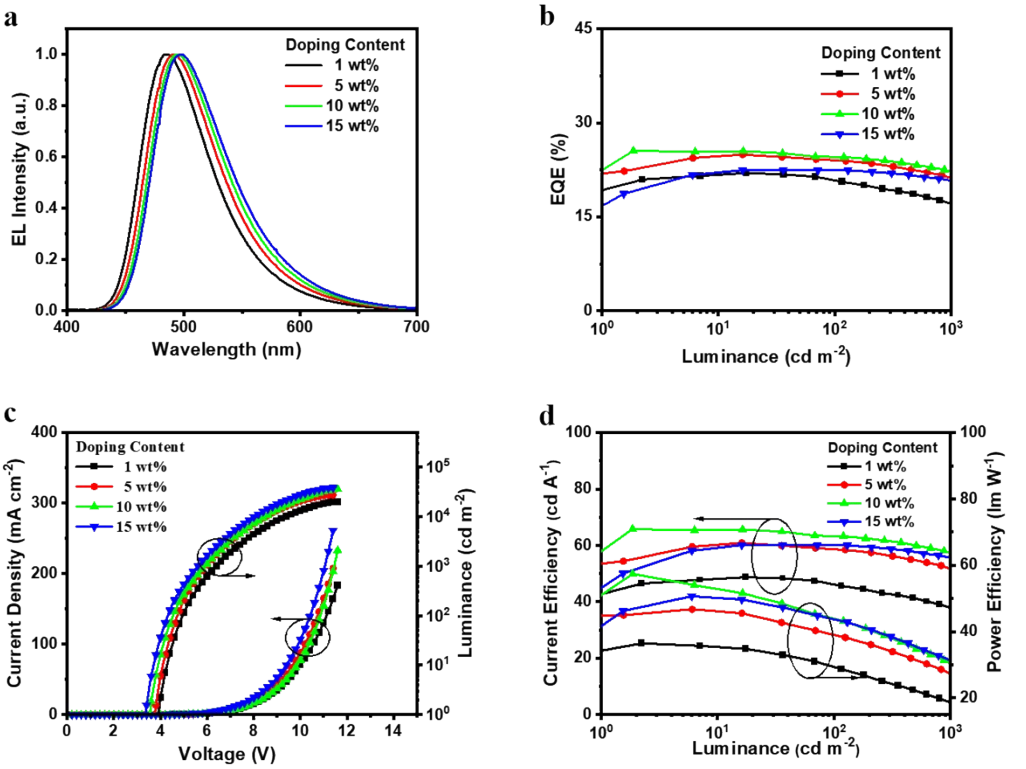

Figure S15. For TMCzSe of different doping contentrations in mCBP, **a.** Normalized EL spectrum; **b.** EQE as a function of luminance; **c.** Current density-voltage-luminance characteristics; **d.** Current efficiency and power efficiency as a function of luminance.

NMR spectra

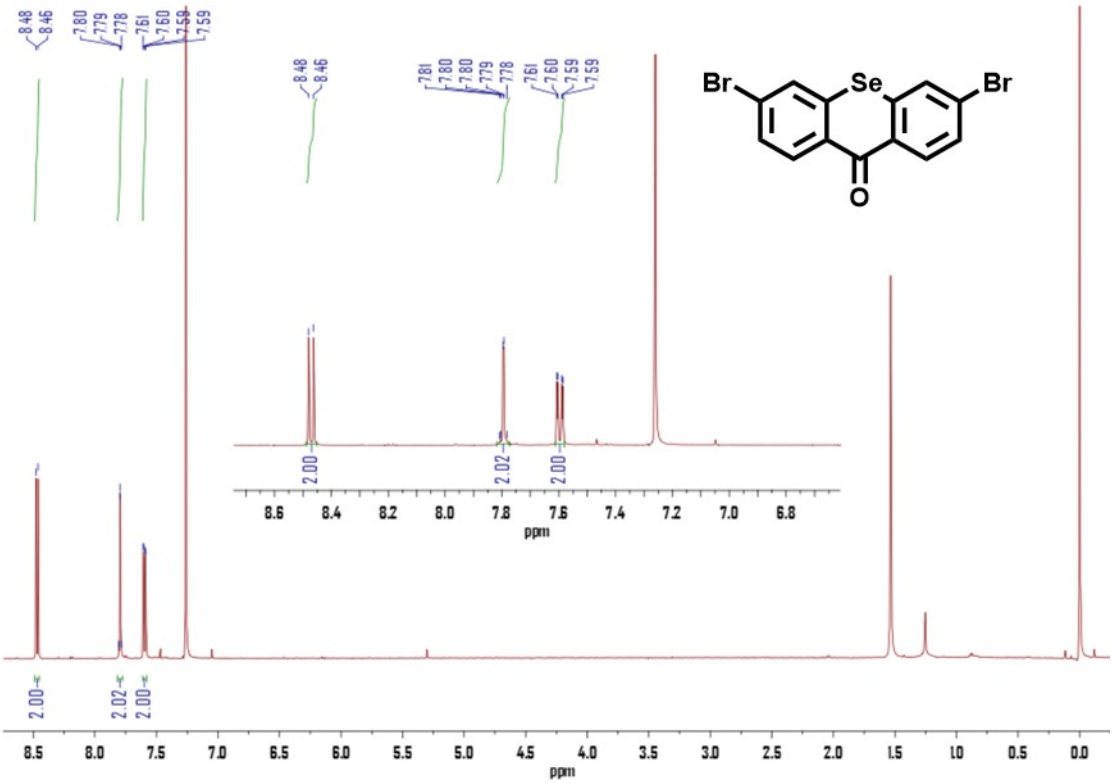

Figure S16. ^{1}H NMR of SeX-2Br.

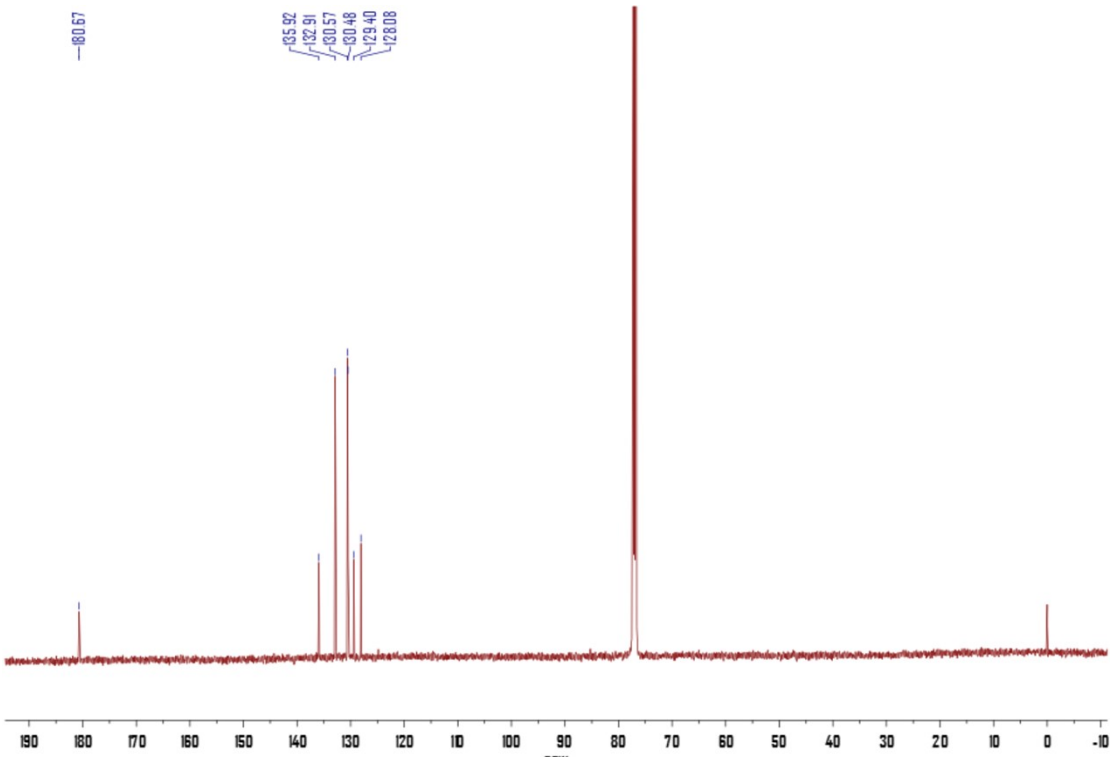

Figure S17. ^{13}C NMR of SeX-2Br.

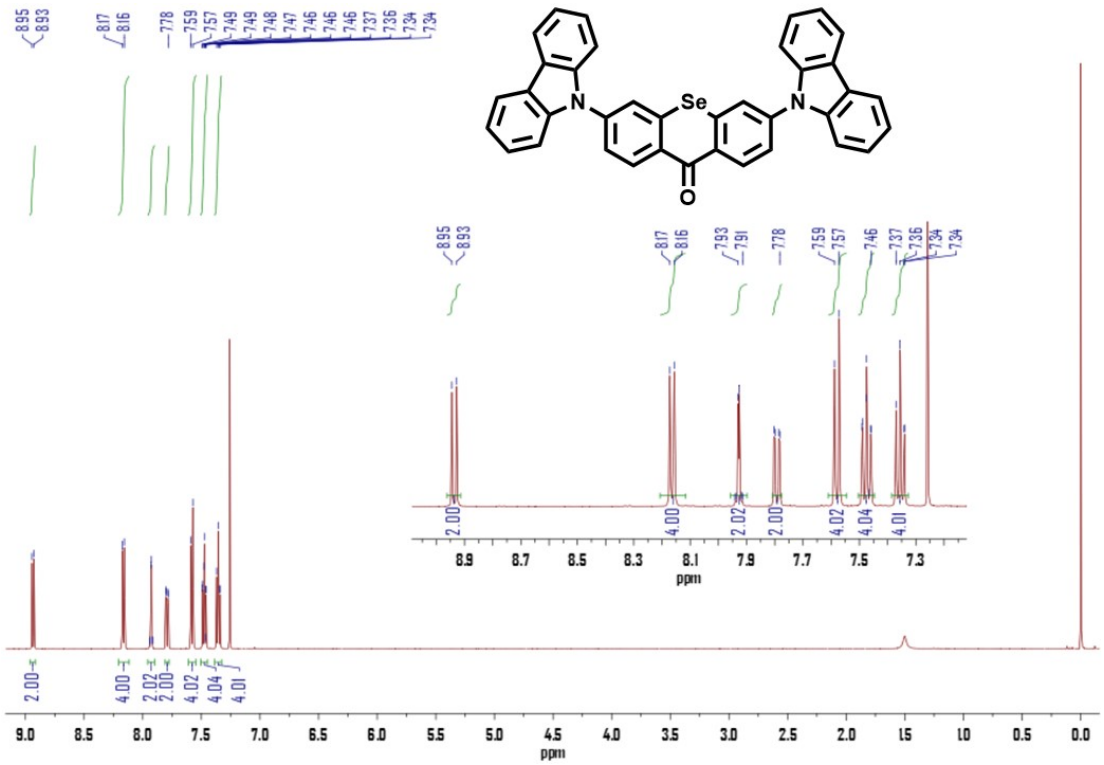

Figure S18. ^{1}H NMR of CzSe.

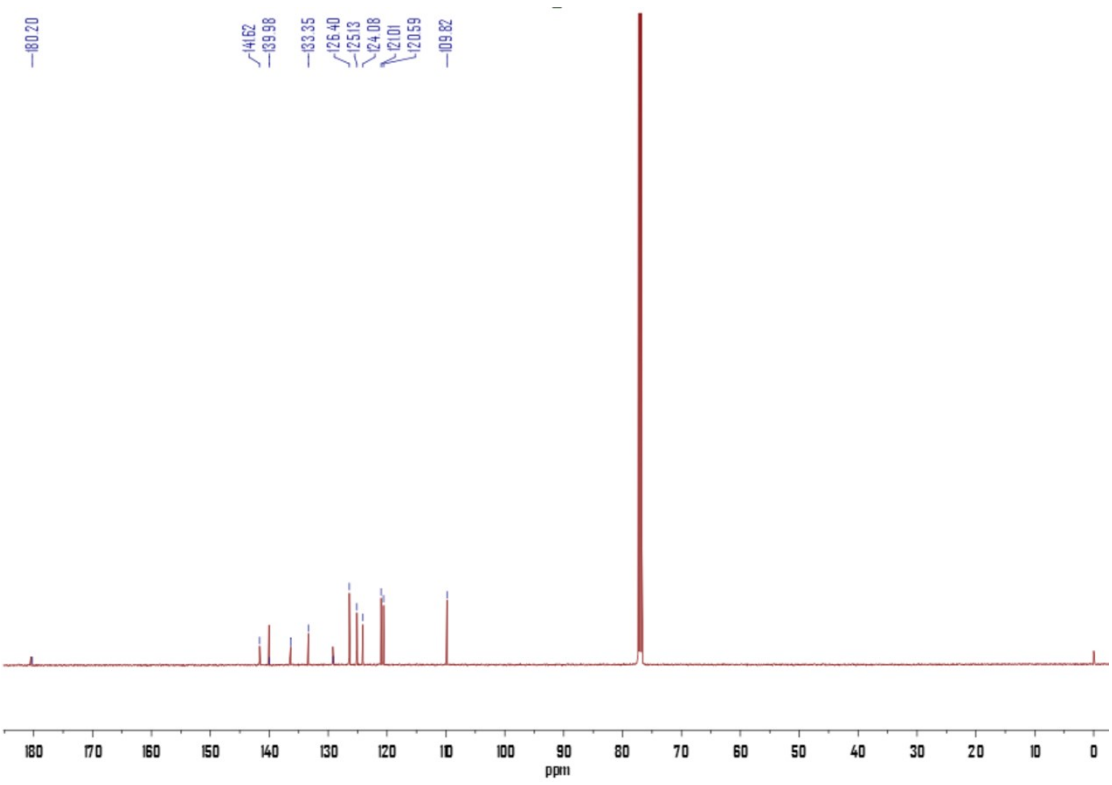

Figure S19. ^{13}C NMR of CzSe.

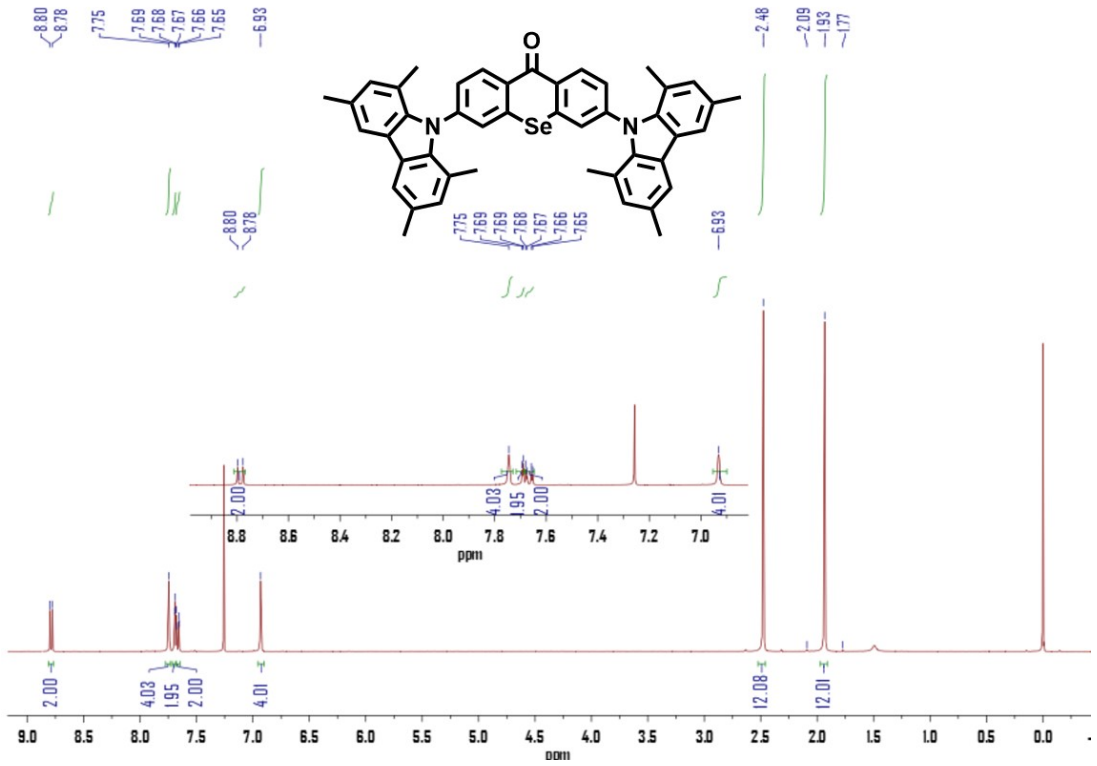

Figure S20. [1]H NMR of TMCzSe.

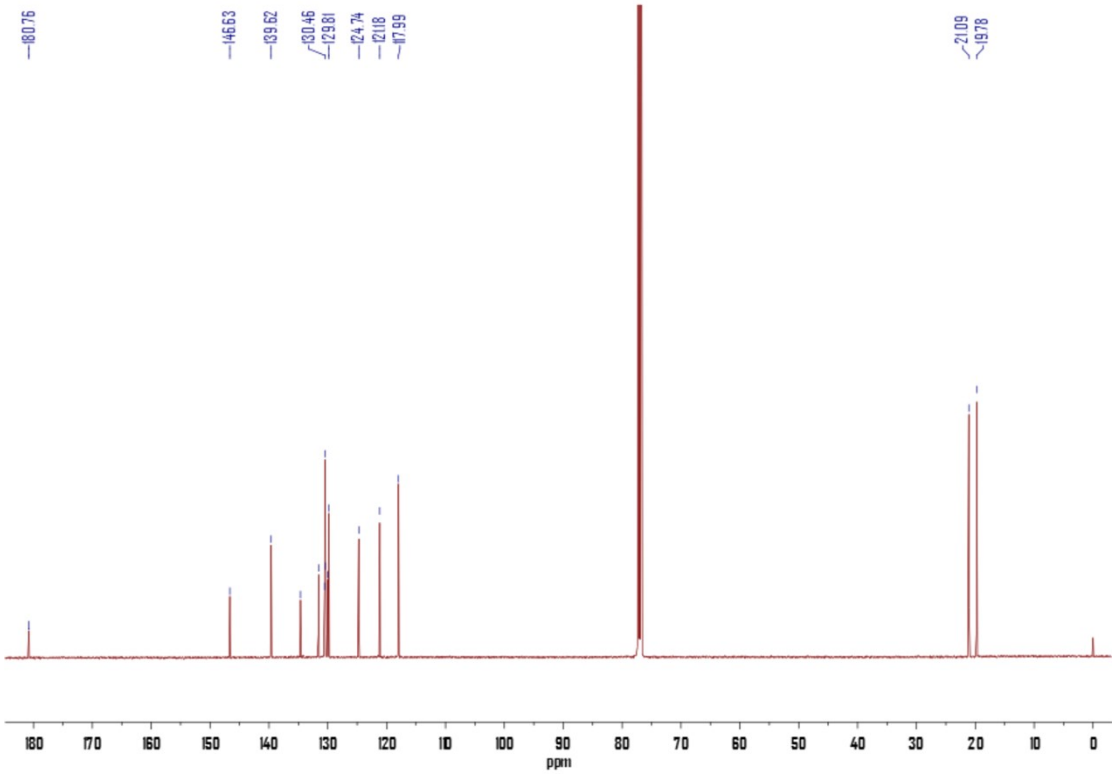

Figure S21. [13]C NMR of TMCzSe.

References

[1] M. J. Frisch, G. W. Trucks, H. B. Schlegel, G. E. Scuseria, M. A. Robb, J. R. Cheeseman, G. Scalmani, V. Barone, B. Mennucci, G. A. Petersson, H. Nakatsuji, M. Caricato, X. Li, H. P. Hratchian, A. F. Izmaylov, J. Bloino, G. Zheng, J. L. Sonnenberg, M. Hada, M. Ehara, K. Toyota, R. Fukuda, J. Hasegawa, M. Ishida, T. Nakajima, Y. Honda, O. Kitao, H. Nakai, T. Vreven, J. A. Montgomery, Jr., J. E. Peralta, F. Ogliaro, M. Bearpark, J. J. Heyd, E. Brothers, K. N. Kudin, V. N. Staroverov, T. Keith, R. Kobayashi, J. Normand, K. Raghavachari, A. Rendell, J. C. Burant, S. S. Iyengar, J. Tomasi, M. Cossi, N. Rega, J. M. Millam, M. Klene, J. E. Knox, J. B. Cross, V. Bakken, C. Adamo, J. Jaramillo, R. Gomperts, R. E. Stratmann, O. Yazyev, A. J. Austin, R. Cammi, C. Pomelli, J. W. Ochterski, R. L. Martin, K. Morokuma, V. G. Zakrzewski, G. A. Voth, P. Salvador, J. J. Dannenberg, S. Dapprich, A. D. Daniels, O. Farkas, J. B. Foresman, J. V. Ortiz, J. Cioslowski and D. J. Fox, Gaussian 09, Revision D.01, Gaussian, Inc., Wallingford CT, 2013.

[2] U. Ekstrom, L. Visscher, R. Bast, A. J. Thorvaldsen and K. Ruud, *J. Chem. Theory Comput.*, 2010, **6**, 1971-1980.

[3] T. Lu, F. and Chen, *J. Comput. Chem*., 2012, **33**, 580-592.

[4] J. Liu, M. Tian, Y. Li, X. Shan, A. Li, K. Lu, M. Fagnoni, S. Protti and X. Zhao, *Eur. J. Org. Chem.*,2020,**47**, 7358–7367.